ONLINE MONITORING OF WHIRL FLUTTER DURING THE ATTILA WIND TUNNEL TESTING

Keith Soal, German Aerospace Center, Göttingen, Germany
Marc Böswald, German Aerospace Center, Göttingen, Germany
Robin Volkmar, German Aerospace Center, Göttingen, Germany
Jan Schwochow, German Aerospace Center, Göttingen, Germany
Martin Tang, German Aerospace Center, Göttingen, Germany
Carsten Thiem, German Aerospace Center, Göttingen, Germany
Alessandro Velo, Leonardo Helicopters, Varese, Italy
Federico Fonte, Leonardo Helicopters, Varese, Italy
Marco Favale, Leonardo Helicopters, Varese, Italy
Stefan van 't Hoff, Royal Netherlands Aerospace Centre, Amsterdam, Netherlands

Abstract

This paper presents the methodology, implementation, and results of an online monitoring system (OLM) for whirl flutter during wind tunnel testing of the ATTILA tiltrotor aeroelastic testbed. The objective was to enable real-time tracking of modal parameters – i.e. frequencies, damping ratios, and mode shapes - under varying operating conditions to safely approach the whirl flutter stability boundary. A robust system combining measurement hardware with automated Operational Modal Analysis (OMA) using the Stochastic Subspace Identification (SSI), supplemented by matrix pencil method, was developed and deployed during the test campaign. Results from multiple configurations revealed amplitude dependent modal behavior and significant structural nonlinearities, particularly in the chord and torsion modes. These nonlinearities were also observed during Ground Vibration Tests (GVT) prior to wind tunnel entry, and required a proper trim of the rotor to limit their impact. The study demonstrates the critical role of real-time system identification and monitoring in identifying aeroelastic stability. It highlights the limitations of forecasts with linear simulation models when the actual hardware shows nonlinear dynamic behavior.

1. INTRODUCTION

Whirl flutter is an aeroelastic instability that can occur in propeller driven aircraft and tiltrotor configurations due to the coupling between aerodynamic, structural, and inertial forces. Consequently, whirl flutter is a important topic in the design of tilt-rotor configurations. These are vertical take-off and landing (VTOL) vehicles, where rotors with collective and cyclic rotor blade pitch control are installed at the wing tips. To better understand and mitigate whirl flutter for future VTOL concepts, wind tunnel tests were conducted in the ATTILA project to support the validation of the NGCTR-TD design, along with testing methods and simulation models. The ATTILA (Advanced Testbed for TILtrotor Aeroelastics) project focused on developing, building, and testing a platform for aeroelastic wind tunnel experiments on tiltrotor aircraft, see Ref. 1 and Ref. 2 for more details. The centerpiece of the project was an instrumented, aeroelastically scaled half-wing with a powered proprotor, see Figure 1. The project required partners with a diverse range of skills, including model design and manufacturing, piloting, wind tunnel operation, modelling and simulation, and stability monitoring. The project consortium consisted of the Royal Netherlands Aerospace Centre (NLR), the German-Dutch Wind Tunnels (DNW), the Polytechnic University of Milan (POLIMI), Leonardo Helicopters (LHD) and the German Aerospace Center (DLR).

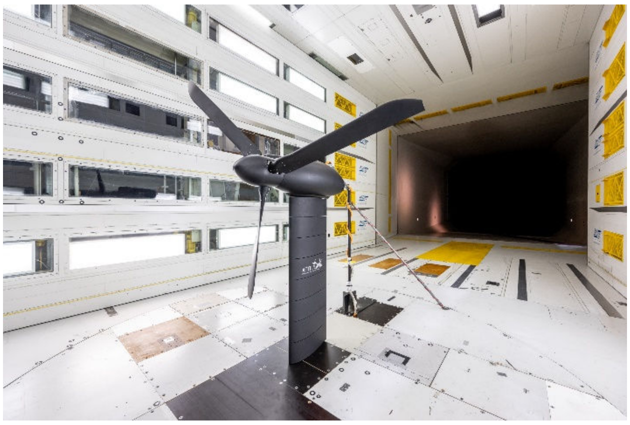

Figure 1 ATTILA whirl flutter test bench in the DNW-LLF

In this work, the results of an online monitoring system (OLM) for modal parameters will be presented. Firstly, the OLM setup regarding hardware and software will be discussed. Then the results of the ground vibration test (GVT) conducted in the wind tunnel will be shown with focus on the identified non-linearities and the implications these had on the wind tunnel test. The testing strategy will then be presented, including excitation types (ambient, sweeps and dwells), modal parameter identification algorithms (stochastic subspace identification and matrix pencil methods), safety limits and test success criteria. Finally, the results of the mode tracking will be presented.

2. GROUND VIBRATION TEST

Prior to the wind tunnel tests, a ground vibration test (GVT) was conducted to characterize the modal behavior of the wing and nacelle model under wind-off conditions. This test was performed in the preparation room with the model already mounted on the test section floor of the wind tunnel to ensure that the boundary conditions were accurately represented. Figure *2* shows the model in test conditions. The wing root was clamped creating a cantilevered beam. The nacelle includes a tilting hinge allowing the tilting degree of freedom. The tilting is constrained by the downstop component, which connect the tilting part of the nacelle with the non-tilting one and then provide stiffness to the nacelle pitch degree of freedom. Two different versions of the downstop component were produced and testsed, the first one was a stiff version, aimed at representing the nominal configuration of the full scale aircraft named downstop-on. A second, more flexible, sping was tested which represented the intermediate conditions when the pylon conversion actuator alone is providing stiffness to the nacelle pitch. The latter configuration is called downstop-off.

For this test, internal accelerometers are used. A total of 29 sensors are used: Seventeen are on the wing, six are on the nacelle, and six are at the wing-nacelle interface. Electrodynamic shakers excite the structure and enable control of the excitation force level. Swept sine excitation at various force amplitude levels is used to characterize the structure's nonlinear response. Different excitation locations are chosen to appropriately excite all modes. Therefore, the model has been excited at the wing and nacelle in different directions.

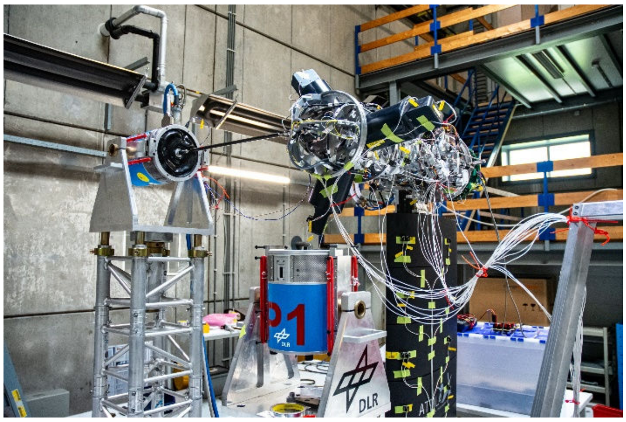

Figure 2 GVT of the ATTILA testbench in the model preparation facility

This modal survey identified approx. 20 modes. Particular attention was given to expected flutter critical modes. It was found that the properties of the torsion mode vary with different excitation amplitudes, exhibiting nonlinear behavior. Figure 3 presents normalized Frequency Response Functions (FRFs) for the swept sine excitation of the torsion mode with the downstop off. The peak around the normalized frequency 1 corresponds to the wing torsion mode response. For higher excitation levels, the peak shifts to lower frequencies. Therefore, higher force excitation and thus higher response amplitudes result in lower eigenfrequencies and lower damping ratios. Figure 4 illustrates the evolution of the normalized modal properties with respect to the excitation force level. Drops of nearly 10% and 40% are observed respectively in the eigenfrequency and damping ratio.

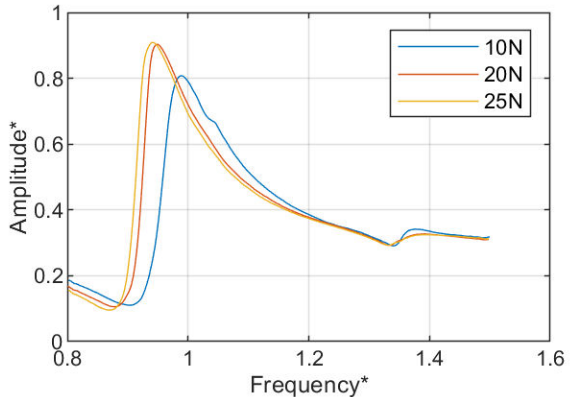

Figure 3 FRF with downstop off at different excitation levels

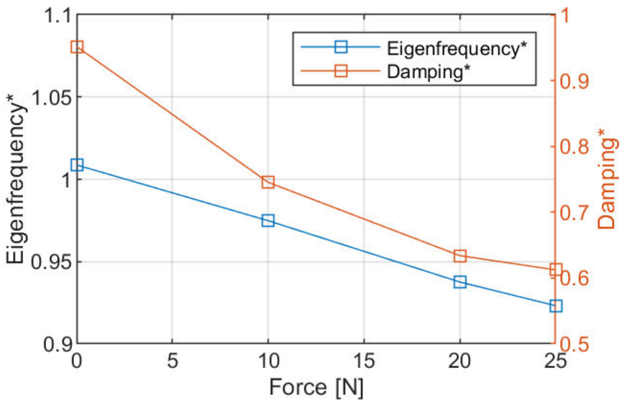

Figure 4 Nonlinearity plot for the torsion mode

This was a very important insight prior to conducting the wind tunnel test. The dependence of the modal behavior on the excitation amplitudes of the wing-pylon structure implies that nonlinear behavior will also occur in the complete aeroelastic system. Then an amplitude dependent system response is expected.

3. ONLINE MONITORING OF WHIRL FLUTTER SETUP

The online-monitoring system (OLM) was developed by DLR combining sensors, data acquisition hardware with software for signal processing, operational modal analysis, tracking and data fusion as follows.

3.1. Hardware setup

The system hardware for the ATTILA wind tunnel test consisted of uniaxial and triaxial piezoelectric acceleration sensors connected to the wing and nacelle. The use of MEMs sensors, strain gauges, fiber optic sensors, load balances or digital image correlation (DIC) data have also been tested and represent possible inputs to the OLM system. A 24 bit commercial data acquisition system was used for digitizing the analog signals as well as sharing synchronization signals with other measurement systems. A real-time data interface was developed in the DLR SASTools software for fetching the data from the commercial measurement system to the OLM software running in Matlab. Several interfaces for different data acquisition systems are available for the OLM tool suiting different applications.

3.2. Software

The OLM software runs in Matlab. The data is acquired in real time and the corresponding data samples are available as data arrays in the Matlab workspace. This allows for continuous signal processing, operational modal analysis and mode tracking. The Matlab parallel processing toolbox is used to optimize the computing resources. The mathematical operations of the algorithms have been optimized for real time performance Ref. 3, Ref. 4 and Ref. 5. A GUI was developed to enable engineers to monitor the aeroelastic stability through different plots showing time data, response spectra, OMA stabilization diagrams, mode tracking over external parameters, Modal Assurance Criteria (MAC) and mode shape plots among others. The results from the OLM tool are written to an SQL data base, and a data base visualization tool allows trend identification and stability extrapolation using the bootstrapping method. An overview of the bootstrapping uncertainty estimation applied to the ATTILA data can be found in Ref. 6. The OLM setup used for the whirl flutter wind tunnel test in DWN-LLF in Marknesse can be seen in Figure 5. The first screen shows the data acquisition software. Screens two and three show two instances of the OLM tool running in parallel. This allows one engineer to experiment with different OMA algorithms and signal processing settings while the second engineer uses a constant setup for result consistency. The fourth and fifth screen show the data base monitoring tool.

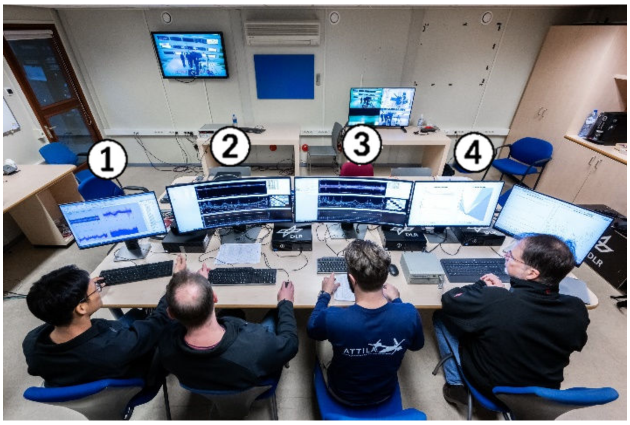

Figure 5 OLM team from DLR monitoring whirl flutter stability in real time

3.3. Algorithms

To enable continuous monitoring of the modal characteristics of the test article, a real-time Operational Modal Analysis (OMA) approach is employed. This method allows for quasi-continuous estimation of eigenfrequencies, damping ratios, and mode shapes based on acceleration response data collected during operation.

The data is processed in a first-in, first-out (FIFO) buffer updated every two seconds, with each update triggering a new OMA identification. This enables the system to track changes in modal parameters in real-time without user intervention. The core identification technique is the Stochastic Subspace Identification (SSI) method, which is well-suited for output-only systems under ambient excitation Ref. 7.

Based on discrete-time state-space modeling, SSI extracts modal parameters from the system's response data using QR projections and singular value decomposition of Hankel matrices. Despite being formulated for linear time-invariant (LTI) systems under stationary excitation, SSI can be applied to slowly varying systems (linear parameter varying, LPV) with acceptable accuracy. However, increased variability in operating conditions may lead to greater uncertainty in the identified parameters. In controlled environments such as wind tunnels, excitation can be maintained sufficiently stationary, minimizing such effects. This methodology provides a robust and automated means for real-time tracking of dynamic system behavior during progressively more critical aeroelastic test conditions.

4. DWELL RESPONSE MONITORING

Alongside the real-time OMA analysis deploying acceleration data, Matrix Pencil Estimation method (MPE) is used to compute flutter trends by analyzing system free decay responses following dwell excitations of the system at resonance. Specifically, signals recorded by the strain bridges on the wing spar, providing root beam bending, chord bending and torsional moments, are considered to estimate modal parameters. The main advantage of this identification approach is that, provided that the system is correctly excited, the target mode is always visible in the system response. On top of that, the response amplitude is visually controllable, which makes the detection of non-linear effects simpler. MPE, here applied as an output-only identification method, relies on the hypothesis that the analyzed system response is a pure free decay, and no further deterministic external force is applied. The method is implemented with stabilization diagram, displaying modal identification results with varying system order. This helps the specialist to distinguish the stable poles from the spurious ones. Hence, each identified pole is associated to a repeatability index, i.e. the rate with which it appears along the considered orders. A detailed discussion of the MPE identification technique can be found in Ref. 6. The Matrix Pencil Method is embedded in the Leonardo Helicopters (LHD) in-house software SIMMPOLE, which allows for signal visualization, processing and system identification.

5. TESTING STRATEGY

The execution of the wind tunnel tests required the cooperation of a team with multiple specialists from different project partners. To this aim special care was devoted in defining the test organization, as already discussed in Ref. 2.

The testing strategy included several aspects including the definition of the test matrix, the success criteria, the responsibility assignment and the communication flow among involved specialists.

A preliminary shakedown wind tunnel tests was instrumental in checking the organization and in improving it in view of the actual test campaign.

5.1. Test Plan

A detailed test plan was defined in support of the test campaign. The test plan was based on the six main operating configurations to be tested, characterized by trim power (power ON / power OFF), downstop configuration (downstop ON / downstop OFF) and by the rotor speed regime (84%NR / 102%NR). The detailed test plan was built on the basis on these configurations and also included the details of the planned tests to be performed at each test point.

The test plan was reviewed each day based on the results progressively gathered and was adjusted based on them. One example was the addition of the rotor gimbal trim angle ad an additional parameter to be studied, on top of parameters listed above.

5.2. Excitation Strategy

The type of system excitation plays a crucial role in accurately identify the modal parameters and improve the certainty of the estimated damping ratio. Two types of excitation were tested: sine sweeps and sine dwells. The benefit of the sweep is that it does not depend on specifying the correct target frequency or and thus does not require a subsequent tuning of it. The disadvantage of sweeps compared to dwells are that they are not possible to perform in-flight without fly-by-wire control systems, as well as limited durations if the aircraft needs to dive to achieve maximum dive speed Vd. A comparison of a sweep and a dwell auto power spectral densities are shown in Figure *6*. Both diagrams show acceleration response spectra. The effect of the rotor fundamental rotation speed and its harmonics can clearly be observed. In the lower frequency range, additional resonance peaks caused by the modes of the system can be observed. In the upper diagram, specifically the frequency range exited by the sweep can be observed directly below the spectral line of the fundamental harmonic of the rotor speed.

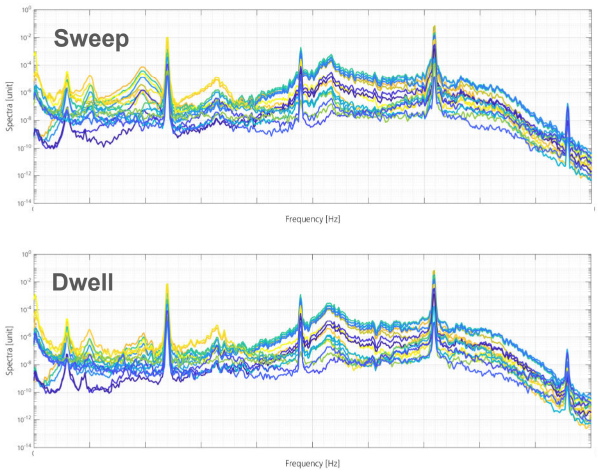

Figure 6 Sweep vs Dwell APSD

A testing strategy was developed using both sweeps and dwells. The sweeps were used to identify the target mode frequency using SSI from the OLM tool at the desired wind speed in real time. The identified eigenfrequency was then communicated as the target frequency for the definition of dwells. The first tests revealed some variability of the identified modal frequency with respect of the excitation amplitude, it was then decided to directly inject three different dwells whose frequencies differed one from the other by 0.1Hz, in this way it was more likely to get a low error between the dwell frequency and the identified frequency even before completing the data process and identification analysis. An example of this strategy can be seen in the spectrogram of Figure *7*. Here one can see two up-sweeps (P110, P110a), a down-sweep (P110b) followed by several dwells.

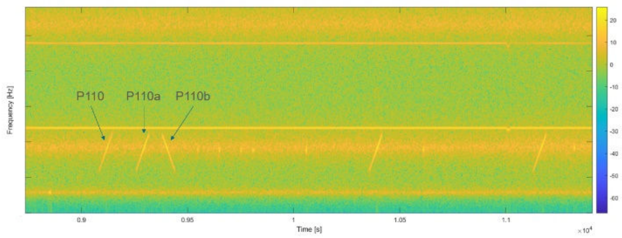

Figure 7 Spectrogram showing sweep and dwell excitation strategy

The result of mode tracking across the entire wind-on data set from the shakedown test can be seen in Figure 8. Here 3 minute data windows were analysed with SSI resulting in 936 mode sets. It can be seen that the Bending (purple) and Chord (blue) modes are well identified throughout the shakedown test regardless of ambient or forced excitation. The Torsion mode is not always well excited by ambient wind and powered rotation. Three clusters of the torsion mode, labelled T1, T2, T3, can be identified, with frequency decreasing while increasing the wind speed. The 1/rev is also identified with almost zero damping. The pylon yaw mode is also identified, though with smaller consistency, being not well excited by ambient excitation.

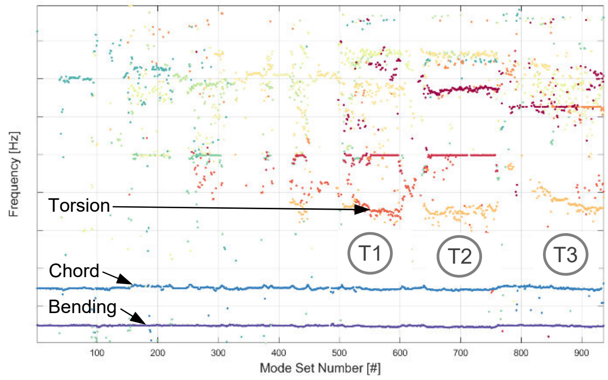

Figure 8 Wind on scatter plot during shakedown test

5.3. Decision Making Framework

The aeroelastic dynamic stability of the model was to be ensured through a decision-making framework that applies to continuation or abortion of the wind tunnel tests. This framework was based on several criteria determined from numerical simulations, measured shakedown test data, as well as previous experience in wind tunnel and flight test campaigns of aeroelastic configurations. The dynamic stability framework consisted of the following criteria:

- On-line structural safety factor monitoring and current safety-factor
- Application of multiple system identification algorithms (i.e. modal parameter estimators) in real-time
- Identified damping ratios provided from these algorithms
- Damping uncertainties
- Logarithmic decrement thresholds
- Averaged spectral amplitudes

An overview of the decision making framework is shown in Figure 9.

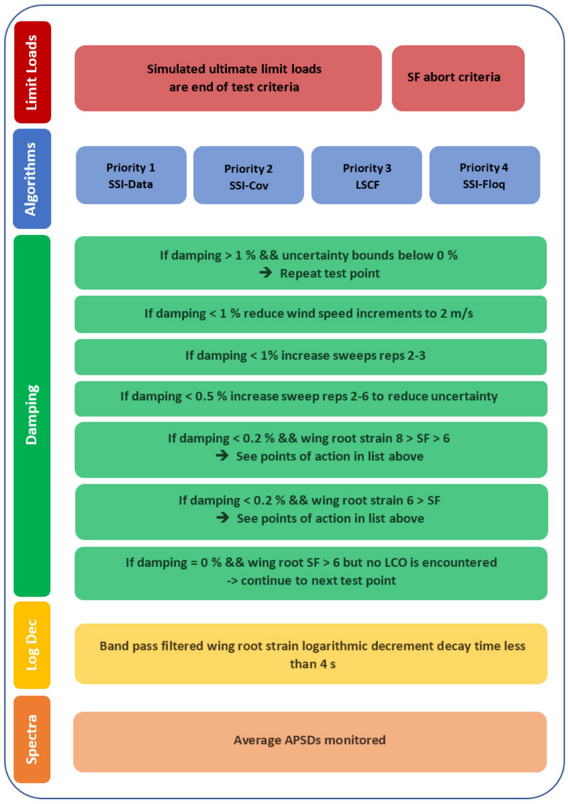

Figure 9 Decision making framework to conclude whether to continue or abort the test

5.4. Success criteria

In order to determine if the wind tunnel test sequence of a given configuration was successful (i.e. a test objective formulated before the test was reached) two metrics were proposed, namely the time to half amplitude and the estimated damping. This makes the evaluation of success more robust and reliable in the absence of a ground truth. The success criterion was defined as having a time-to-half-amplitude of the whirl flutter critical mode larger than a defined value. The equivalent damping ratio was calculated based on the following equation for damping as a function of time to half amplitude:

$$d = \frac{\ln(2)}{(2*\pi*f_n*T_d)} \quad (1)$$

Where d is the damping ratio, f_n is the natural frequency, and T_d is the decay time. The selected damping thresholds was then 0.3% for the torsion mode and 0.55% for the chord mode.

To limit the impact of noise in estimated time-to-half-amplitude and damping, it was also imposed that the two conditions were considered only when the signal-to-noise ratio was higher than 5.

6. WIND TUNNEL TEST RESULTS

This section presents the experimental findings from the ATTILA whirl flutter test campaign. The tests were conducted to investigate the aeroelastic stability characteristics of the system under varying configurations and operating conditions. The primary focus lies on the onset and progression of the stability observed in the chord and torsion modes. By systematically varying the model configurations, excitation types, and tunnel operating conditions, a controlled and incremental approach to the stability boundary was achieved.

The results from two configurations will be presented in this section. These are shown in the following table and will be referred to as C4 and C6.

Configuration	Power	Downstop	Gimbal
C4	OFF	ON	2°
C6	OFF	OFF	2°

6.1. Configuration C4: Time data, spectra and stabilization diagrams

Initial testing of C4 with gimbal angle 0° started at a wind speed of 20.6 m/s and progressed up toto 108 m/s without reaching identified damping values under 0.3 %. Instability occurred when the angle of incidence of the full model was changed This strong dependence of the system stability on the rotor tilting was not predicted by numerical model and investigated in Ref 10 and Ref 12 and is attributed to the effect of friction in rotorhead components, that acts differently between condition with zero rotor tilting angle and conditions with nonzero rotor tilt angle. Configuration C4 was then tested with 1°, 2° and 3° gimbal angle. The results for the most critical condition of gimbal angle 2° are presented here.

The acceleration time data measured on the wing and nacelle can be seen in Figure 10. The four discrete wind speeds of 61.7 m/s, 77.2 m/s, 90 m/s and 95.2 m/s can clearly be seen due to the increasing random-like vibration response levels.

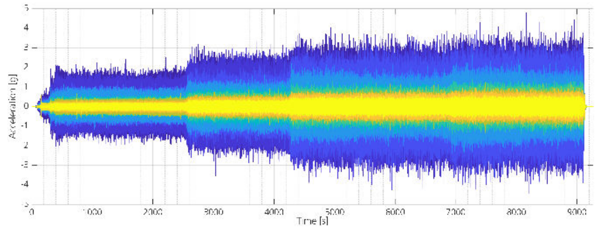

Figure 10 Acceleration time data from the wing and nacelle at 4 discrete wind speeds.

Due to the non-linearity of the system as found during the GVT, the type and amplitude of excitation have an influence on the modal parameters, and therefore on the aeroelastic stability. For SSI the sine sweeps provided the best input, based on the lowest uncertainty in the identified modal parameters. This is due to their ability to excite discrete frequencies in a desired band with sufficient energy, especially when the target mode is unknown at a given wind speed or configuration. The Auto Power Spectral Densities (APSDs) calculated using the Welch method (Ref. 8), are shown for two different types of excitation in Figure 11 and Figure 12. In Figure 11 a longitudinal (LON) sweep with 60 % amplitude is swept through the bandwidth containing the torsion mode. This excitation type introduces a torsion into the structure therefore targeting the torsion mode. From the APSDs it can be seen that this mode and frequency band are well excited as the amplitude levels are about 10^2 above the levels in the adjacent non-excited frequency bands.

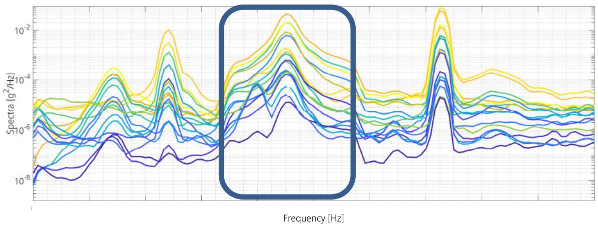

Figure 11 APSDs from LON sine sweep with 60% amplitude targeting torsion mode

In Figure *12* a collective (COLL) sine sweep with 40% amplitude is used to target the chord mode. Here it can also be seen from the amplitudes of the APSDs that the chord mode is well excited. The amplitude of excitation is also an important factor since the damping ratio is affected by it. The amplitude was chosen based on the highest possible excitation allowing the measured loads not to exceed the safety factors of the ultimate load limits.

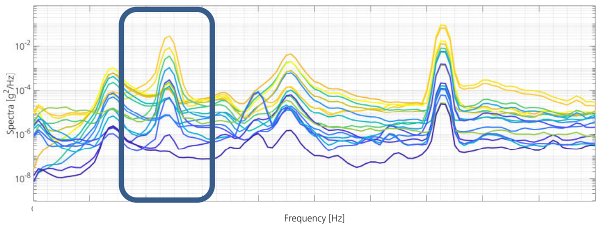

Figure 12 APSDs from COLL sine sweep with 40% amplitude targeting chord mode

The results from modal analysis using SSI are shown in the stabilization diagrams in Figure 13 and Figure 14. The bending, chord and torsion modes are identified from both excitation types, however the torsion mode is identified more clearly from the longitudinal cyclic (LON) excitation and the chord mode from the collective excitation. The measured (dashed red) vs synthesized (dashed blue) spectra are also seen to match well. The 1/rev frequency of the rotor is identified by SSI with almost 0 % damping as the fourth peak in Figure *13*. The 1/rev is not identified during the collective sweep in Figure *14*, however due to the time domain formulation of the algorithm, this does not have an effect on the neighboring modes.

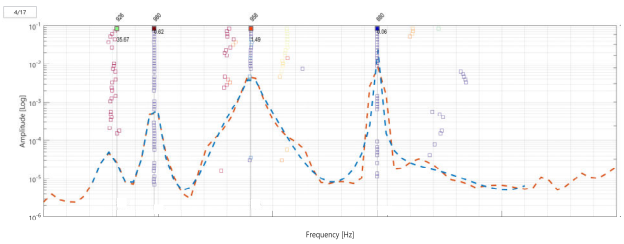

Figure 13 Stabilization diagram from LON sine sweep with 60% amplitude targeting torsion mode

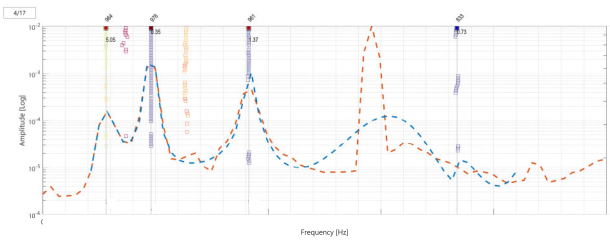

Figure 14 Stabilization diagram from COLL sine sweep with 40% amplitude targeting chord mode

The identified mode shapes or eigenvectors resulting from SSI are shown in Figure *15*. Here one can see the bending [a], chord [b], torsion [c] and pylon yaw [c] modes. Mode shape components can be seen on the wing with 17 channels in total. The acceleration sensors on the nacelle were excluded from the system identification due to the lower signal to noise ratio compared to the acceleration sensors in the wing.

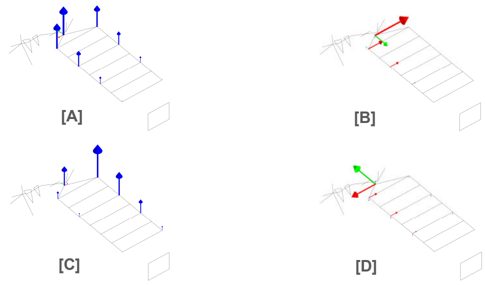

Figure 15 Identified mode shapes [a] bending [b] chord [c] torsion [d] pylon yaw

6.2. Configuration C4: Modal analysis and tracking

The results from modal analysis using SSI for the bending (blue), chord (red) and torsion (yellow) modes can be seen in Figure 16. The frequency as a function of wind speed is shown above and the damping as a function of wind speed is shown below. The results at each discrete wind speed are plotted using box and whisker plots showing the mean and standard deviation. Here it can be seen that the aeroelastic damping of the bending mode is high, ranging from 10 % to 40 %, and shows the well-known trend of increasing with increasing wind speed in the absence of modal coupling. The aeroelastic dampings of the chord and torsion modes are low, under 4 %.

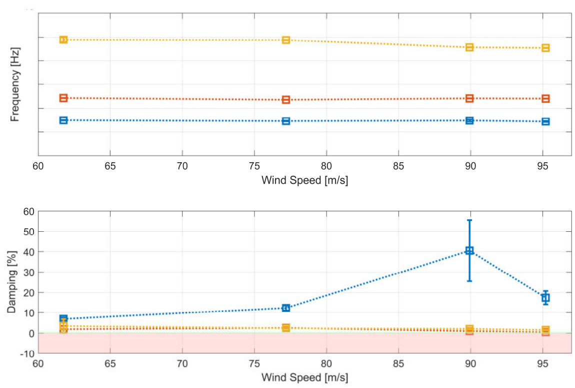

Figure 16 Modal analysis and tracking using SSI for bending (blue), chord (red) and torsion (yellow) modes showing both frequency and damping as a function of wind speed

The damping trends are studied in more detail by isolating the chord and torsion modes in Figure 17. The success criteria of 0.55 % for chord mode is indicated by the green shaded area, while the unstable region is indicated by the red shaded area. It can be seen that at 61.7 m/s the chord mode is more lightly damped with ~2 % damping compared to the torsion mode ~3.8 % damping. The damping of the chord mode then increases at 77.2 m/s while the torsion decreases. With increasing wind speed both the chord and torsion damping ratios decrease with the chord mode reaching the test success criteria first with 0.44 % damping and std 0.23 %. The chord mode is therefore found to become unstable first.

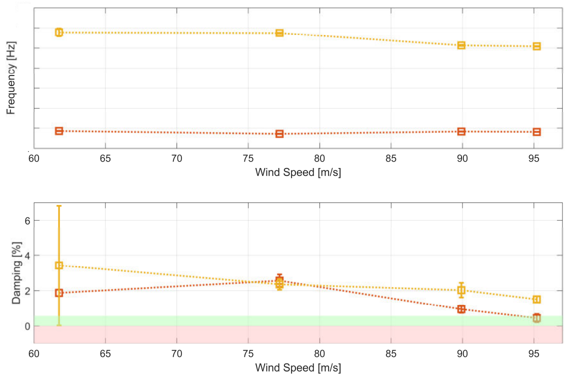

Figure 17 Modal analysis and tracking using SSI of chord and torsion modes only

6.3. Configuration C6: Time data, spectrogram, modal analysis and tracking

Significant wearing of the blade pitch sensors was observed while performing the tests in C6 configuration. For this reason tests were interrupted and the sensors were cleaned so to reduce friction. Testing in C6 configuration was then resumed and the data gathered after the pitch sensor cleaning are shown by the subplots in Figure *18*. The measured time histories of the acceleration responses show four discrete events. The vibration modes and rotor 1/rev can be seen from the intensity signatures in the spectrogram. The first three lines from the bottom of the spectrogram indicate the bending, chord and torsion modes respectively. The fourth line shows the rotor 1/rev.

Since the low-speed portion of the test matrix in C6 configuration had already been performed, only spot checks were conducted to avoid the time-consuming full envelope expansion procedure of the test envelope with small speed increments.

The piloting approach use for moving from one point to the following one consisted in first reducing the rotor speed, then increase wind tunnel speed and finally to increase again rotor speed up to the desired value. Once the rotor speed stabilized the dynamic tests for the desired point were executed. This approach was chosen so to avoid possible rotor overspeed during wind tunnel speed increase. The change in rotor speed is visible from the spectrogram in Figure *18*.

The focus of the following data analysis will be on the block measured between approx. 1400 s and 1600 s. This corresponds to constant wind speed of 92.6 m/s with increasing rotor 1/rev to its nominal value. The the level of the acceleration response is seen to ramp up in the upper diagram during this event before the wind is turned off by case of emergency. From the spectrogram the rotor 1/rev is first decreased, the wind speed is increased and the rotor 1/rev is then seen to be increased back to the nominal value.

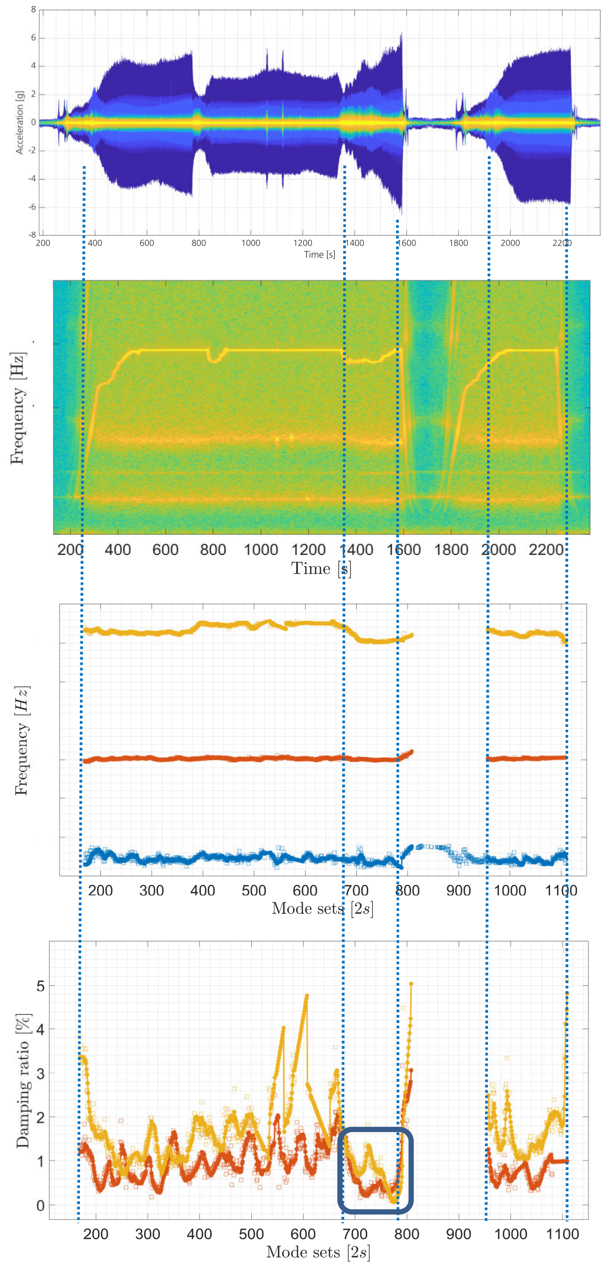

Figure 18 Whirl flutter results from C6.1 showing time data, spectrogram, frequency and damping

The modal analysis results from SSI for frequency and damping are shown in the lower two diagrams of Figure *18* by small squares, together with the Kalman filter data fusion, see Ref. 9, shown by the solid lines and circles. The modes are well identified with OMA even without any commanded excitation. The frequencies of the bending, chord and torsion modes can be seen, with a notable decrease by about 5 % in the torsion mode frequency (yellow).

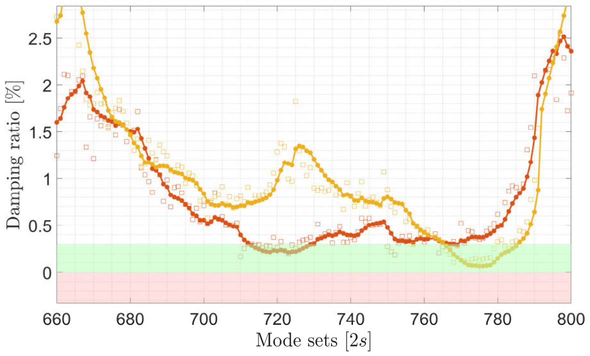

Figure 19 Damping ratio of the chord mode in red and the torsion mode in yellow in the zoomed block above

The diagram of the damping ratios shows that the damping of the chord mode (red) is in general lower than the damping of the torsion mode (yellow). By zooming in on the identified mode sets in the critical time interval, see Figure 19, one can see that the chord and torsion modes both already show very low damping with still decreasing trends as the 1/rev is increased. The chord mode (red) drops below the torsion damping threshold of 0.3 %, which is considered as one of the success criteria. It then however stops decreasing while the torsion mode (yellow) afterwards drops below the 0.3 % threshold and gets very close to the whirl flutter stability boundary before the knock-it-off command was given by the test director and the wind speed was rapidly reduced. This shows that for the power off and downstop off configuration the torsion mode is demonstrated to become unstable first.

7. Numerical Model Predictions

Numerical whirl flutter simulations were performed using three aeromechanical modelling frameworks: FLIGHTLAB, MASST/CAMRADII, and MBDyn/DUST as shown in Ref. 10. Each model was built using a combination of structural and aerodynamic modelling techniques and tuned afterwards using pre-test Ground Vibration Test (GVT) data. The comparison between predicted and identified frequencies and damping are shown for the Chord mode in *Figure 20* and the Torsion mode in *Figure 21*. In these figures, the damping ratios are shown for the simulation results by the blue, red and green curves. The experimental results from the MPE and SSI algorithms are shown by the yellow and purple error bars. It can be seen that the CAMRADII and FLIGHLAB models incorrectly predict that the torsion mode becomes unstable first. The experimental results from MPE and SSI do not match exactly, however this can be attributed not only to the different identification algorithm, but also to the non-linear behaviour of the model and therefore the damping ratios are highly dependent on the amplitude and type of excitation. Nevertheless, both experimental methods agree that the Chord mode is the critical mode for Configuration C4, that is the mode with lower flutter speed, and agree well when the damping ratios are low i.e. the mode is well excited.

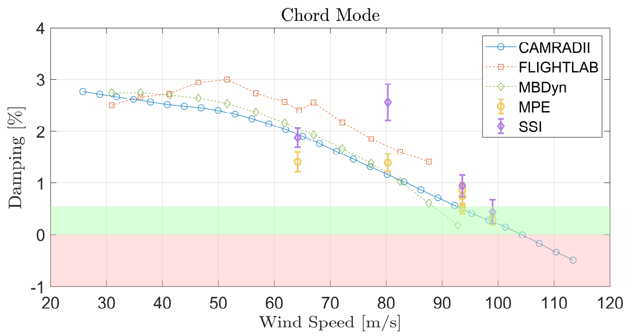

Figure 20 Simulation vs experimental results for chord mode damping; power off, downstop on, conversion mode rpm, 2° gimbal pitch (C4)

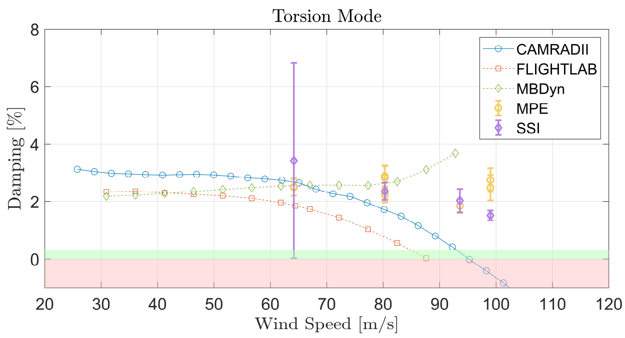

Figure 21 Simulation vs experimental results for torsion mode damping; power off, downstop on, conversion mode rpm, 2° gimbal pitch (C4)

It can be seen that the numerical models provide conservative estimates for the damping of the torsion mode, which was predicted to be the critical mode instead of the chord mode. These discrepancies can be attributed to multiple factors that also include nonlinearities in the physical testbed, such as friction in the rotorhead components (both the pitch and gimbal bearings) and amplitude-dependent damping behavior, see Ref. 11 for further information on this phenomena., which are not fully captured by the linear assumptions inherent in the simulation models. For example, the strong sensitivity of the chord mode damping to gimbal trim angle, observed experimentally, was not predicted by the numerical models. Subsequent sensitivity studies described in Ref. 10 showed that introducing simplified representations of friction in the rotorhead improved the correlation, suggesting that the dependence on rotor tilt angle can be attributed to friction.

8. CONCLUSIONS

Observations from the test results led to the following conclusions:

1. Even if thorough simulations have been performed all modes around the band of interest should be directly targeted with excitation due to non-linear system behavior.

    ❖ Directly excite all modes of interest

2. Excitation signals should be improved using multiple sweeps rather than single sweeps through the target frequency. This results in better observability. and also allows uncertainty estimation using bootstrapping.

    ❖ Use multiple sweeps

3. Excitation amplitudes should be varied from 40 %, 60 %, 80 % as close to the limit load safety factor as possible to explore non-linear amplitude dependent system response.

    ❖ Vary the excitation amplitude

4. Use sweeps to identify the target frequency for dwells. If the dwell frequency is not well selected, the non-linear modes will not be excited.

    ❖ Use sweeps in combination with dwells

5. Filter for excitation type and amplitude to identify consistent trends due to non-linear system behavior.

Author contact:

Keith Soal Keith.Soal@dlr.de
Marc Böswald, Marc.Boeswald@dlr.de
Robin Volkmar, Robin.Volkmar@dlr.de
Jan Schwochow, Jan.Schwochow@dlr.de
Martin Tang, Martin.Tang@dlr.de
Carsten Thiem, Carsten.Thiem@dlr.de
Federico Fonte Federico.Fonte@leonardo.com
Alessandro Velo Alessandro.Velo@leonardo.com
Marco Favale Marco.Favale@leonardo.com
Stefan van ‘t Hoff Stefan.Van.t.Hoff@nlr.nl

9. ACKNOWLEDGMENTS

The authors give thanks to the complete ATTILA team for their contributions to the success of the test campaign. This research received funding from the Clean Sky 2 – H2020 Framework Program, under grant agreement N. 863418 (the ATTILA project).

10. REFERENCES

1. Van ‘t Hoff, S., Van Vilsteren, J., Cocco, A. and Masarati, P., “Design of a Tiltrotor Semi-Span Wind Tunnel Model for Whirl Flutter Investigations”, AIAA SciTech 2023 Forum, National Harbor, Maryland, January, 2023.
2. Van ‘t Hoff, S., Fonte, F., Soal, K., Schneider, O., and Kapteijn, K, “Whirl Flutter Testing of ATTILA Tiltrotor Testbed – Initial Results,” Vertical Flight Society 80th Annual Forum, Montréal, Québec, Canada, May, 2024.
3. Volkmar R. et al. “Experimental and operational modal analysis: Automated system identification for safety-critical applications”. In: Mechanical Systems and Signal Processing 183 (2023), p. 109658. issn: 0888-3270
4. Soal K. et al. (2024) *Flutter flight testing: Using operational modal analysis to identify, track and predict flutter for safe and efficient flight test campaigns.* International Forum on Aeroelasticity and Structural Dynamics, IFASD 2024, 2024-06-17 - 2024-06-20, Den Haag, Niederlande.
5. Böswald M. et al. Online monitoring of flutter stability during wind tunnel testing of an elastic wing with pylon and engine nacelle within the HMAE1 project. International Forum on Aeroelasticity and Structural Dynamics 2019, IFASD 2019 2019.
6. Velo, A., Fonte, F., Favale, M., Soal, K., Böswald, M., Volkmar, R., and Schwochow, J., "Uncertainty Estimation in Experimental Whirl Flutter Modes Identification." 81st International Annual Forum, Vertical Flight Society, VFS 2025.
7. Van Overschee, P., & De Moor, B. Subspace identification for linear systems: Theory—Implementation—Applications. Springer 1996.
8. Welch PD. The Use of Fast Fourier Transform for the Estimation of Power Spectra: A Method Based on Time Averaging Over Short, Modified Periodigrams. IEEE Transactions on Audio and Electroacoustics AU-15 (2):70-73. 1967.
9. Volkmar R, Sinske J, Soal KI, Govers Y, Böswald M. Reliable monitoring of modal parameters during a flight vibration test using autonomous modal analysis and a Kalman filter. IFASD 2024.
10. Van ‘t Hoff, S., Fonte F., Velo A., De Vita P., Cassoni G., and Masarati P. "ATTILA Tiltrotor

Whirl Flutter Code-to-Test Correlation." 81st International Annual Forum Vertical Flight Society VFS 2025.
11. Worden, K., and Tomlinson, G.R. Nonlinearity in Structural Dynamics: Detection, Identification and Modelling. Institute of Physics Publishing. 2001.
12. De Vita, P., et al. “Tiltrotor Wind-Tunnel Model Whirl Flutter With Mid-Fidelity Aerodynamics and Mechanical Friction”. European Rotorcraft Forum, Venice, Italy, 9-12 September 2025